Preprints.org

Article

A Crucial Role of Proteolysis in Formation of Intracellular Dinitrosyl Iron Complexes

Karolina E. Wójciuk [*] , Jarosław Sadło , Hanna Lewandowska , Marcin Kruszewski

Article

A Crucial Role of Proteolysis in Formation of Intracellular Dinitrosyl Iron Complexes

Karolina E. Wójciuk [1,2,*], Jarosław Sadło [3], Hanna Lewandowska [2,4] and Marcin Kruszewski [2,5]

[1] Nuclear Facilities Operations Department, National Centre for Nuclear Research (NCBJ, Otwock, Poland

[2] Department of Radiobiology and Biological Dosimetry, Institute of Nuclear Chemistry and Technology, Dorodna 16, 03-195 Warsaw, Poland

[3] Department of Radiation Chemistry and Technology, Institute of Nuclear Chemistry and Technology, Dorodna 16, 03-195 Warsaw, Poland

[4] School of Health & Medical Sciences, University of Economics and Human Sciences in Warsaw, 59 Okopowa St., 01-043 Warsaw, Poland

[5] Department of Molecular Biology and Translational Research, Institute of Rural Health, Jaczewskiego 2, 20-090 Lublin, Poland

* Correspondence: karolina.wojciuk@ncbj.gov.pl

Abstract: Dinitrosyl iron complexes (DNICs) stabilize nitric oxide in cells and tissues and constitute an important form of its storage and transportation. DNICs may comprise low-molecular-weight ligands, e.g. thiols, imidazole groups in chemical compounds with low molecular weight (LMWDNICs) or high-molecular-weight ligands, e.g. peptides or proteins (HMWDNICs). The aim of this study was to investigate the role of low- and high-molecular-weight ligands in DNICs formation. Lysosomal and proteasomal proteolysis was inhibited by specific inhibitors. Experiments were conducted on human erythroid K562 cells and on K562 cells overexpressing heavy chain of ferritin (FERH). Cell cultures were treated with •NO donor. DNICs formation was monitored by electron paramagnetic resonance (EPR). Pretreatment of cells with proteolysis inhibitors diminished intensity and changed shape of DNICs specific EPR signal in a treatment time-dependent manner. The level of DNIC formation was significantly influenced by the presence of protein degradation products. Interestingly, formation of HMWDNICs depended on the availability of LMWDNICs. The extent of glutathione involvement in the in vivo formation of DNICs is minor yet noticeable, aligning with our prior research findings.

Keywords: K562 cells; electron paramagnetic resonance; nitric oxide; reactive nitrogen species; dinitrosyl iron complexes; chelatable iron; glutathione

1. Introduction

An important reaction involving nitric oxide (•NO) within living cells is its interaction with iron and specific biological ligands, including proteins, peptides, and amino acids [1,2]. The interaction results in the formation of dinitrosyl iron complexes (DNICs) characterized by electron paramagnetic resonance (EPR)-detectable $g_\perp$ = 2.04 and $g_\parallel$ = 2.014 signals (the so-called 2.03 signals, in accordance with the average value of its g-factor [1]). DNICs formation was observed in cells and tissues exposed to endogenous [3] or exogenous •NO [4]. The nature of biological ligands forming DNICs and their interactions are not well understood. EPR analysis of frozen solutions revealed that the anisotropy of g values of formed DNICs displays significant variations depending on geometry, electronic structure and molecular weight of involved ligands, and is an important indicator of ligand type and the complex structure. Nitrite and •NO can react with heme and non-heme iron proteins to form DNICs, however, kinetics of in vivo formation and distinctions between DNICs derived from nitrite or •NO remains unclear [5]. During formation of DNICs a chelatable iron might be also sequestered, resulting in an iron-starved phenotype. Thus, DNICs formation affects cellular iron homeostasis and alters activity of iron-containing proteins, but also reduces the pro-oxidant capacity of cells [3].

DNICs formation may involve a variety of iron-containing proteins, such as those comprising iron-sulfur centers [6–8], heme groups [9] or non-heme iron [8,10,11]. Some examples of proteins that have been shown to form DNIC include mitochondrial aconitase [12–15], ribonucleotide reductase [16], cytochrome c oxidase [17] and nitrogenase [18]. However, the specific proteins that are targeted during DNIC formation can vary depending on the cell type and physiological context [5]. Biosynthesis of DNICs was first discovered in 1964 [19], and continued investigations revealed tetrahedral $[(NO)_2Fe(L)_2]$ complex, as a natural and ubiquitous DNIC formed from interaction of $^\bullet NO$ with non-heme iron-sulphur ([Fe-S]) proteins and cellular labile iron pool [8,20–34].

DNICs involvement in various $^\bullet NO$-mediated cellular and organismal functions has been described in several reviews [8,35]. There is an increasing awareness of the biological role of DNICs, and this warrants further studies on DNICs structure and on the pre-requirements for their biosynthesis. DNICs have been proposed as a "working form" of $^\bullet NO$ under physiological conditions [19]. On the other hand, high-molecular-weight DNICs (HMWDNICs) accumulate in lipoprotein aggregates that contain partially hydrophobic fragments, such as lipid bilayers. These complexes are highly stable and inert, as demonstrated by their resistance to decomposition in the presence of iron chelators [36]. HMWDNICs seem to be the most abundant form of DNICs observed in vivo, however this might be biased by the fact that their enhanced stability may contribute to their higher abundance and better detectability in cellular extracts after protein fractionation [37].

The objective of this study was to investigate the contribution of low- (LMW) and high-molecular-weight (HMW) ligands in formation of DNICs. Our previous study revealed that DNICs are formed primarily in the endosomal/lysosomal fraction and degradation of iron-containing metaloproteins is crucial for its formation in vivo [38]. This prompted us to undertake a more detailed investigation on the role of protein degradation in DNICs formation, through the use of proteolysis inhibitors of different specificity.

In this study, K562 human erythroid precursor cells were treated with proteolysis inhibitors followed by treatment with a $^\bullet NO$ donor and DNICs specific signal was recorded with regard to its shape and intensity. In addition, as glutathione appears to be the most abundant low molecular weight thiol ligand, its role in DNICs formation was also investigated.

The function of low molecular weight DNICs (LMWDNICs) as $^\bullet NO$ donors has been observed: administration of LMWDNICs to experimental animals resulted in the formation of high molecular weight protein-bound DNICs (HMWDNICs) due to transfer of $Fe(NO)_2$ groups from added complexes to proteins [39,40].

2. Materials and Methods

Unless otherwise indicated all chemicals were purchased in Sigma-Aldrich (Merck), Poland.

Cell lines and chemicals

K562 human erythroid precursor cells (ATCC CCL-243) were grown in suspension in RPMI-1640 supplemented with 10% foetal bovine serum, 2 mM glutamine and antibiotics in humidified 5% CO_2 incubator to a final density of 10^7 cells per milliliter. One batch of K562 cells was stably transfected with transferrin heavy chain (FERH) sequence containing DNA plasmid by electroporation using the BTX ECM600 apparatus, according to the manufacturer's recommendation. The efficiency of transfection was evaluated using green fluorescent protein (GFP)-encoding plasmids (4.7 kbp; p-EGFP-N1) co transfected with FERH vector. The transfected cell lines were designated K562/FERH.

Inhibition of proteolysis

The cells were treated with the following inhibitors: 15 mM of ammonium chloride (lysosome inhibitor; Sigma Aldrich - Germany), 100 µg/mL of leupeptin (lysosome inhibitor; Sigma), 50 µM ALLM (N-acetyl-L-leucyl-L-leucyl-L-methioninal; lysosome inhibitor; Sigma - Germany), 20 µM lactacystin (proteasome inhibitor; Sigma - Germany), 25 µM MG-132 (Z-Leu-Leu-Leu-al; proteasome

inhibitor, Sigma - Germany), 50 μM MG-101 (ALLN, N-acetyl-L-leucyl-L-leucyl-L-norleucinal, a calpain and cathepsin inhibitor; Sigma - Germany) or 5 μM MG-262 (Z-Leu-Leu-Leu-B(OH)$_2$; proteasome inhibitor; BioMol - Germany). NO donor was added to generate DNICs.

Generation of DNICs

After 2, 4 or 6 hours of treatment with proteolysis inhibitor in the complete medium at 37°C, the cells were treated with •NO donor (diethylammonium (Z)-1-(N,N-diethylamino)diazen-1-ium-1,2-diolate, DEANO) for 15 min at 37 °C, at concentration 70μM. The final ˙NO concentration in the culture medium was 100 μM). The donor spontaneously dissociates in a pH dependent, first-order process with a half-life of 2 min at 37°C, pH 7.4. Untreated cells served as a reference.

EPR measurements

DNICs formation was monitored by electron paramagnetic resonance (EPR). Samples were prepared according to the following procedure: NO-treated cells were centrifuged for 10 min at 250 x g, resuspended in 200 μL of PBS buffer and flash-frozen in liquid nitrogen. EPR spectra were measured on an X-band Bruker 300e spectrometer. All spectra were recorded at 77 K with microwave power of 1 mW and modulation amplitude of 3 G, time constant 41 ms. The characteristic EPR signals corresponding to DNICs formation were obtained. Once the EPR signal intensity had been measured, the protein concentration in each sample was assayed by the Bradford method [41].

Preparation of subcellular fractions

To investigate the role of ligands in DNICs formation in various cellular compartments, cell homogenates were treated with DEANO and fractionated by differential centrifugation. Approximately 10^8 cells were washed with phosphate-buffered saline (PBS) and pelleted at 300 x g for 10 min. The pellet was resuspended in the ice-cold buffer A (250mM sucrose; 1mM EDTA; 20mM N-(2-hydroxyethyl)piperazine-N'-ethanesulfonic acid) and broken in a Potter-Elvehjem homogenizer. The homogenate was centrifuged through the Centricon centrifugal filter devices (Amicon) with cut-off values: 100000 MWCO (molecular weight of ligands < 100 kDa) and 30000 MWCO (molecular weight of ligands <30 kDa) at 1,000 x g for 10 min. EPR spectra were recorded for each fraction separately and recalculated for protein content.

Glutathione and thiol determination

A total content of compounds containing thiol groups was measured fluorometrically with the use of monobromobimane (MBB, Sigma Aldrich), a non-fluorescent bimane dye that adds a fluorescent tag when reacting with thiol groups (Ex/Em of thiol conjugate = 380/475 nm). The cellular GSH content was also measured fluorometrically, but with the use of monochlorobimane (MCB, Sigma Aldrich), a bimane dye, specific for glutathione even in the presence of other thiol groups (Ex/Em of glutathione conjugate = 380/460 nm) [42].

In some experiments, to lower the cellular glutathione content, approx. 25 x 10^6 of cells were incubated for 24 h at 37°C in in 25 mL complete medium containing 200 μM D,L-buthionine [S,R]-sulfoximine (BSO), a γ-glutamylcysteine synthetase inhibitor. In yet another series of experiments, to increase the cellular glutathione content the cells were incubated with 10 mM N-acetylcysteine (NAC), a glutathione synthesis precursor, in the same conditions. After incubation, DEANO was added to generate DNIC, and EPR signal was recoded and recalculated for protein content measured by the Bradford method.

Statistical evaluation

The significance of differences between the mean values was analyzed by a pairwise comparison using Student's t-test for independent samples.

3. Results and discussion

Cellular proteins that might serve as a HMW-ligands, are degraded either in lysosomes, cytoplasmic organelles containing various types of proteases active at acidic pH, or targeted for degradation to proteasomes in a ubiquitin-dependent process, both processes easy to control using appropriate inhibitors. On the other hand, a level of the main potential LMW peptide ligand, glutathione, can be also controlled by the use of a specific precursor (NAC) or inhibitor (BSO) of its synthesis. In other words, the use of specific proteolysis inhibitors allows for elucidation of the role of HMW-ligands, whereas controlling the glutathione level allows for elucidation of the role of LMW-ligands in DNICs formation. The study also aimed to understand the relationship between both types of protein ligands in DNICs formation in various cellular compartments.

To further elucidate the role of HMW-ligands in intracellular DNIC formation, their cellular content was increased by the use of ferritin-overexpressing cells. Ferritin, is an iron storage protein known to promote DNICs formation [43]. Thus, we aimed to explore how overabundance of HMW protein, such as ferritin, may affect the formation and stability of DNICs.

The effect of inhibitors of lysosomal proteolysis on DNICs formation

To estimate whether proteins degraded in the lysosome pathway are a source of DNICs components, we used ammonium chloride, which effectively inhibits lysosomal proteases by alkalization of the lysosome interior. Pretreatment of K562 cells with 10 mM NH_4Cl induced a time-dependent decrease in DNICs formation (Figure 1). The result shows that proteins degraded in the lysosomes are an important source of DNICs components.
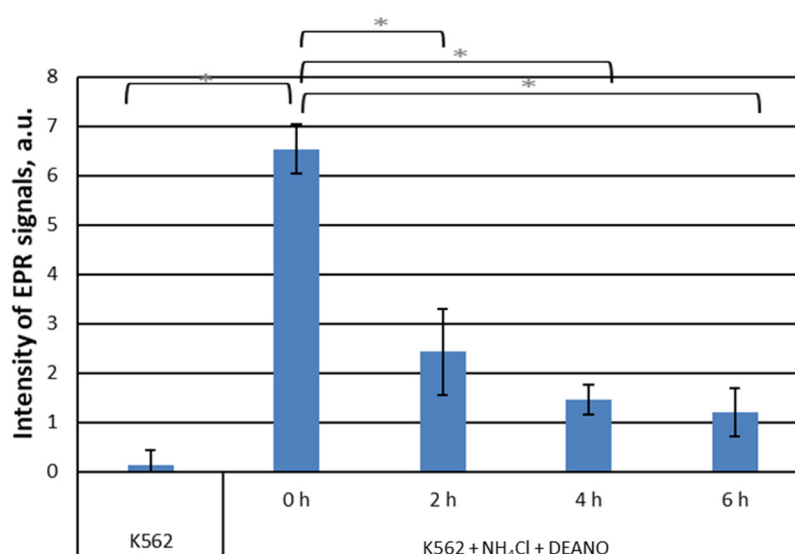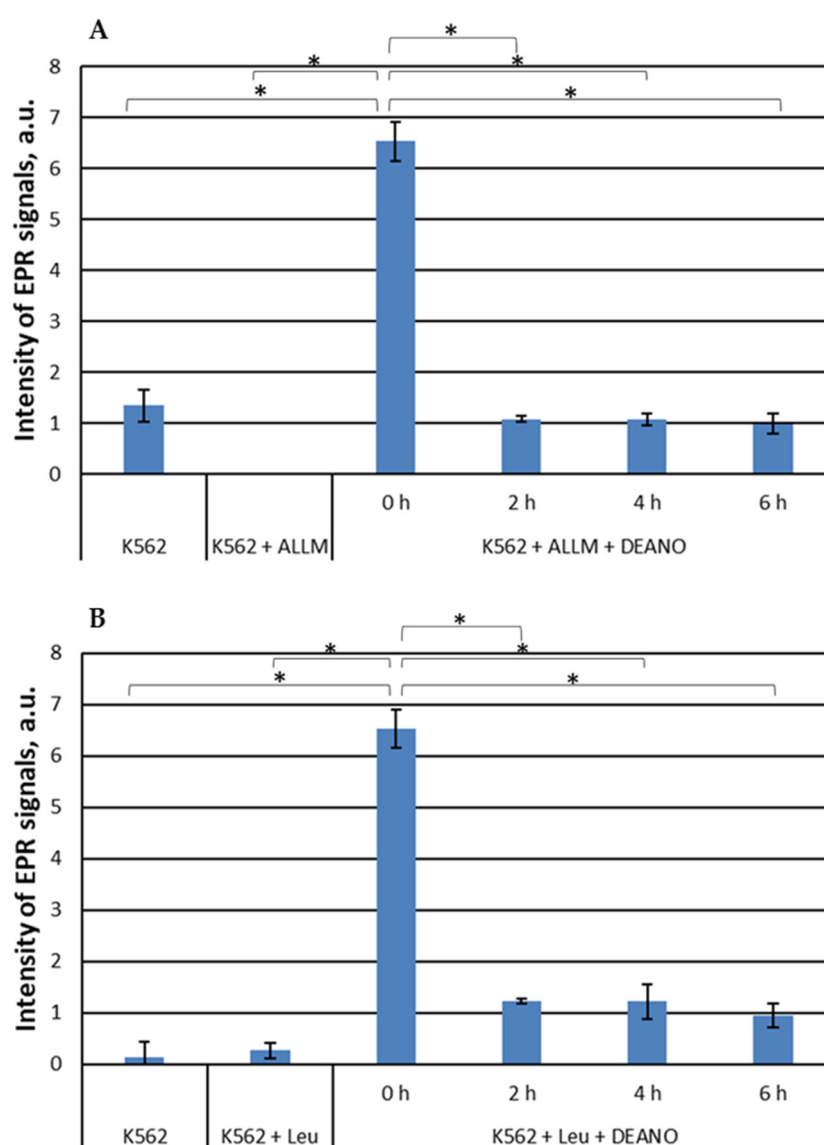

Figure 1. EPR signal induction in K562 cells incubated with 15 mM NH_4Cl for indicated time (0, 2, 4, 6 h) and then treated with 70 µM DEANO for 15 min at 37°C; mean ± SD, n=3, * denotes statistically significant difference, $P < 0.05$.

Further, two other proteolysis inhibitors were applied: ALLM (N-acetyl-L-leucyl-L-leucyl-L-methioninal) [44] or leupeptin (N-acetyl-L-leucyl-L-leucyl-L-argininal). ALLM, binds the active site of cysteine proteases, mainly calpains and cathepsins, and forms a covalent bond with the catalytic cysteine residue, thereby blocking their activity [45]. Leupeptin is a reversible inhibitor of serine, threonine and cysteine proteases, including cathepsins and calpains. It inhibits protein degradation in lysosomes and cytosol, but it is more potent against lysosomal proteases. Leupeptin also binds the active site of proteases and forms a covalent bond with the catalytic residues, thereby blocking their activity [46]. It has been shown to inhibit autophagy by blocking the breakdown of cellular components in lysosomes [47]. Both inhibitors prevented the formation of DNICs in a similar way,

but unlike in the NH_4Cl treatment, the effect was not time-dependent, and full intensity of inhibition was observed already after 2 h of treatment (Figure 2).

These three inhibitors block primarily the same proteolysis pathway, namely lysosomal pathway, thus we expected similar effect. The observed discrepancy is likely due to the different modes of action. Peptide inhibitors interact directly with the active centers of enzymes, whereas the action of NH_4Cl is indirect, through the alkalization of the intralysosomal environment. Since lysosomal mechanisms maintaining acidic pH are very efficient [48], apparently it takes more time to inhibit lysosomal enzymes.
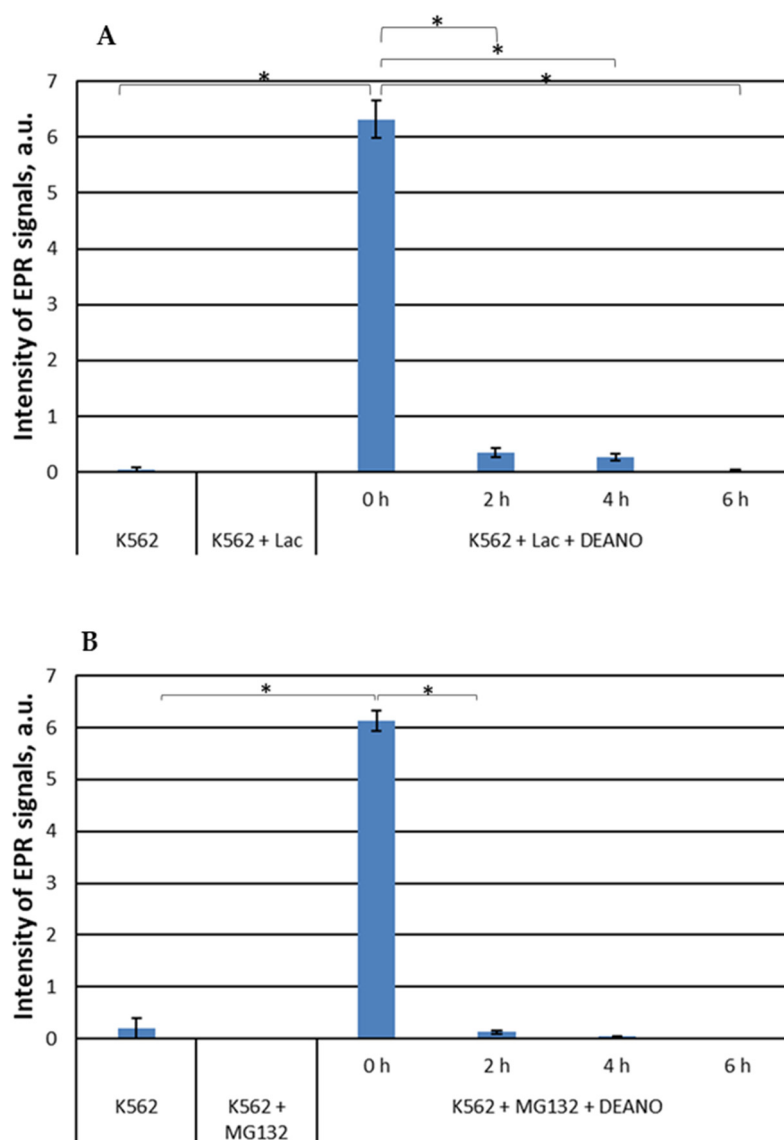

Figure 2. EPR signal induction in K562 cells incubated with 50 μM ALLM (a) or 100 μM leupeptin (b) for indicated time (0, 2, 4, 6 h) and then treated with 70 μM DEANO for 15 min at 37°C; mean ± SD, n=3, * denotes statistically significant difference, $P < 0.05$.

The effect of proteasome inhibitors on DNICs synthesis

To examine the effect of proteasomal proteolysis on DNIC formation, we inhibited proteasome with 20 μM lactacystin (LAC) [49] or 25 μM MG-132 [44,50]. LAC covalently binds the active site N-terminal threonine residue of proteasome β-subunit to form an intermediate species, clasto-lactacystin β-lactone. Consequently, it inhibits proteasome-dependent proteolysis at concentrations of 20 μM or higher [49]. MG-132 is a specific, potent, reversible and cell-permeable proteasome inhibitor that reduces degradation of ubiquitin-conjugated proteins by the 26S complex without

affecting its ATPase and isopeptidase activities [51–53]. This substrate-mimicking peptide acts primarily on the chymotrypsin-like site in the β subunit of proteasome. Both inhibitors strongly inhibited formation of DNIC in DEANO-treated K562 cells. Extremely low or no EPR signals were detected indicating that the treatment with proteasome inhibitors entirely stopped DNICs biosynthesis (Figure 3). This result shows that proteins degraded in proteasomes are a very important source of DNICs components.
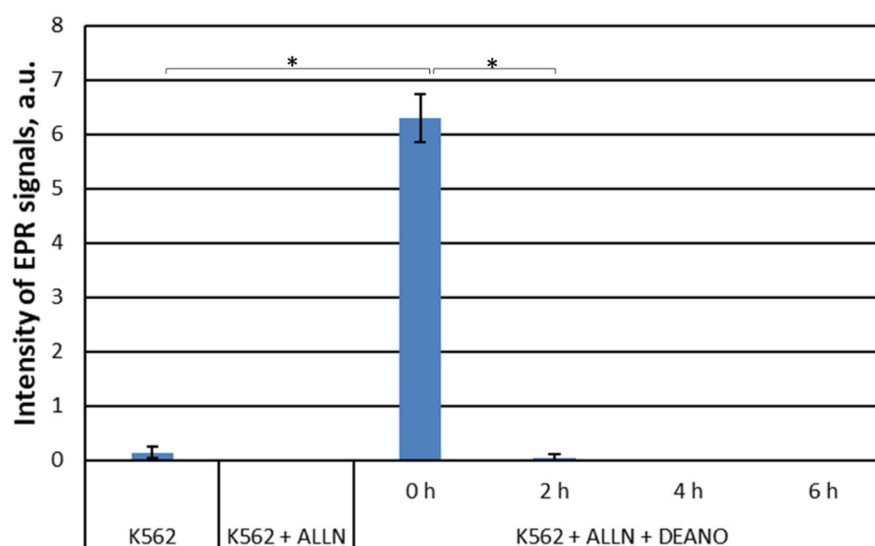

Figure 3. EPR signal induction in K562 cells incubated with 15 mM (a) 20μM lactacystin and (b) 25 μM MG132 for indicated time (0, 2, 4, 6 h) and then treated with 70 μM DEANO for 15 min at 37°C; mean ± SD, n=3, * denotes statistically significant difference, $P < 0.05$.

Effect of the total proteolysis inhibition on DNIC synthesis

Two inhibitors were applied that inhibit all types of cellular proteases, MG-101 and MG-262. MG-101 (N-acetyl-L-leucyl-L-leucyl-L-norleucinal; ALLN) is a cell-permeable inhibitor of calpain I, calpain II, cathepsin and cathepsin L. It inhibits neutral cysteine proteases and the proteasome [44, 50]. MG-262 is a highly potent and selective cell-permeable inhibitor of proteasome [54] and probably lysosome proteolysis [55]. MG-262, a boronic peptide acid, is a potent proteasome inhibitor that selectively and reversibly inhibits the chymotryptic activity of the proteasome [56, 57], while leupeptin inhibits serine, cysteine and threonine proteases but it does not inhibit α-chymotrypsin or thrombin. Leupeptin is a competitive transition state inhibitor and its inhibition

may be relieved by an excess of substrate [58, 59]. The experiments revealed that total inhibition of the cellular proteolysis obtained with these inhibitors completely prevented DNICs formation. As both inhibitors gave identical results, only results for ALLN are shown (Figure 3).

Figure 4. EPR signal induction in K562 cells incubated with 20μM ALLN for indicated time (0, 2, 4, 6 h) and then treated with 70 μM DEANO for 15 min at 37°C; mean ± SD, n=3, * denotes statistically significant difference, $P < 0.05$.

The effect of glutathione concentration modulation on DNICs synthesis

One of the aims of our studies was to evaluate the role of LMW thiol ligands in DNICs formation. Hence, the contribution of glutathione (GSH) in DNICs formation in K562 cells was evaluated. The cellular GSH content was modulated by treatment with N-acetylcysteine (NAC), which stimulates GSH synthesis by maintaining a high free cysteine pool, or by treatment with D,L-buthionine [S,R]-sulfoximine (BSO), a specific inhibitor of γ-glutamylcysteine ligase, the first enzyme of glutathione synthesis pathway.

As shown in Figure 5, treatment with DEANO did not affect cellular glutathione level. However, 24 h treatment with NAC stimulated glutathione synthesis and significantly increased its level roughly by 40%. In contrary, treatment with BSO, as expected, decreased the glutathione level, again roughly by 60%.

To examine the role of glutathione in DNICs formation, cell cultures pretreated with NAC or BSO were subsequently treated with DEANO, and intensity of EPR signal was compared with cells treated with DEANO alone. Despite big differences in glutathione level (Figure 5), the intensity of EPR signal in DEANO-treated cells did not differ substantially neither in cells with increased glutathione level (NAC treated) nor in cells with decreased glutathione level (BSO treated), as compared with not treated cells. However, a statistically significant difference was revealed between NAC- and BSO-treated cells (Figure 6). As the same cell cultures were used to obtain the data presented in Figures 5 and 6, these data suggest that glutathione had only a neglectable role in the formation of intracellular DNICs. Hence, we conclude that the inhibition of proteolysis is the decisive factor limiting the production of DNICs.
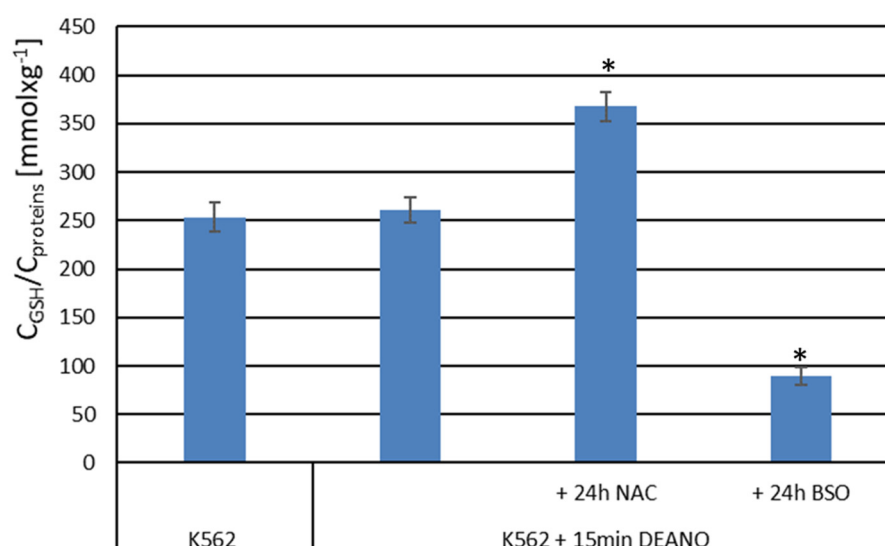
Figure 5. Cellular level of GSH in DEANO-treated cells previously treated with NAC or BSO. GSH levels were estimated with the monochlorobimane method; mean ± SD, n=3; * denotes statistically significant difference versus not treated control cells, $P < 0.05$.
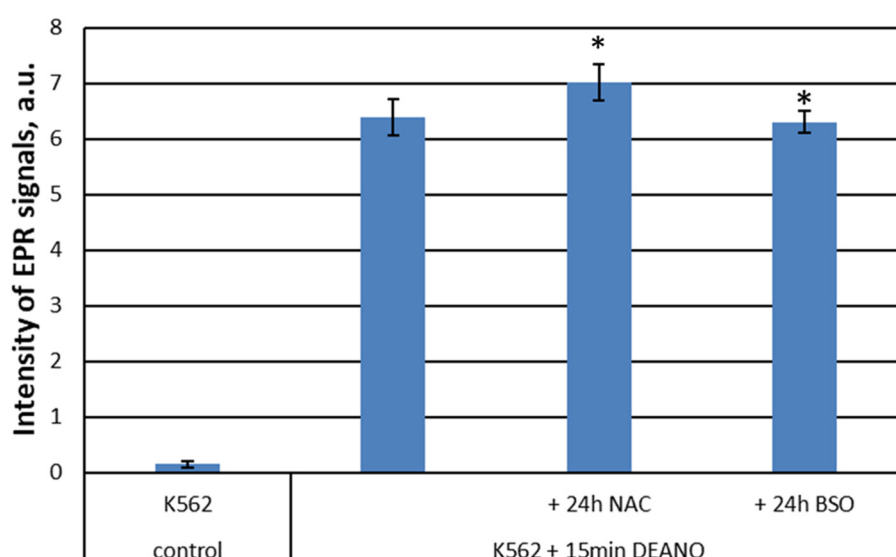
Figure 6. Intensity of EPR signal in cells differing in glutathione level. *denotes statistical significance between the marked levels, $P < 0.05$.

Cellular low and high molecular ligand fractions

The role of low and high molecular ligands in DNICs formation *in vivo* was further examined by cell fractionation. K562 cell homogenate was treated with DEANO and fractionated. The high intensity EPR signal from DNICs was detected in the whole cell lysate and in the cytosol. The cytosol fraction was further fractionated by centrifugal filtration to obtain fraction with ligands < 100 kDa. As expected, centrifugation through the molecular membrane with a cut-off value of 100 kDa eliminated the majority of HMW thiols, with a neglectable effect on glutathione content (Figure 7). With a molecular mass 0.3 kDa the same level of glutathione should be present in all fractions.
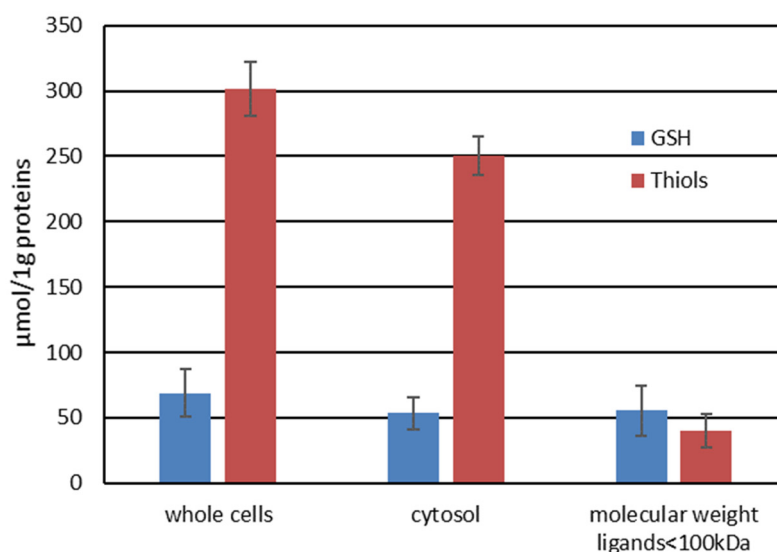
Figure 7. The levels of GSH and total thiols in cellular subfractions.

The intensity of EPR signal dramatically dropped when HMW proteins were filtered out (Figure 8). The EPR signal intensity in <100 kDa fraction was less than 40% of this of unfiltered cytosol. All together these results further support the crucial role of HMW ligands in formation of DNICs.
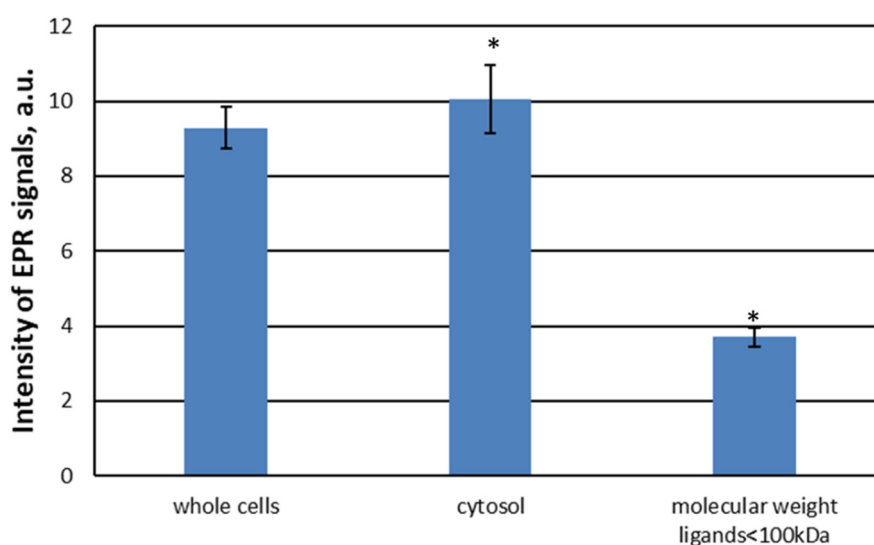
**Figure 8.** The intensity of the EPR signal in individual cell fractions. Cell homogenate was treated with 70 μM DEANO.

Characterization of EPR signal of protein-bound DNICs

LMWDNICs, which are not bound to proteins, exhibit a symmetrical EPR signal at room temperature with a g-value of 2.03. Hyperfine Structure (HFS) analysis of the EPR signal of DNICs with cysteine showed that these complexes contain pairs of molecules of cysteine and NO (nitric oxide). The hyperfine structure (HFS) in the EPR signal at 273K is a result of the interaction between unpaired electron and nitrogen nuclei of NO ligands and protons of cysteine [60]. The signal became narrower as the temperature increased, indicating that these DNICs are highly mobile at higher temperatures, leading to an averaging of the anisotropic properties of the signal [60]. The anisotropic shape of the EPR signal at 273K of DNICs often encountered in biological systems suggests that these DNICs are bound to proteins [60–62].

Prior investigations by Lee et al. [63] laid the groundwork for understanding of EPR signal symmetry in ferritin-bound DNICs. An illustration of how the EPR signal at 77K is effected by specific ligands involved in the formation of protein bound DNICs was provided, demonstrating that the EPR signal of ferritin originated DNIC was a composite of signals from complexes bound either to histidine or cysteine residues of the protein. Notably, these two distinct species generated EPR signal that shared a common central value of approximately 2.03. However, they exhibited dissimilar symmetries, with the histidinyl complex displaying a rhombic symmetry, whereas the cysteinyl complex exhibited an axial symmetry [27,63,64] .

It's also worth noting that the symmetry of the EPR signal can also be influenced by the structural configuration of the protein ligands, as exemplified by the EPR spectra of DNICs associated with different isoforms of glutathione S-transferase [65,66]. Thus, DNICs bound to proteins with only one thiol group, such as bovine or human serum albumin, exhibit lower (rhombic) symmetry, resulting in an EPR signal with three different g-factor values. This decrease in symmetry suggests that DNICs incorporate a ligand, likely a histidine residue of the protein. When these protein-bound DNICs come into contact with an excess of LMW thiols (e.g. cysteine or glutathione), they undergo a reversible transformation, replacing the protein's histidine ligand with the LMW thiol. This change in coordination results in a more axially symmetrical EPR signal. In cells and tissues, it's possible that DNICs can contain either two or one HMW protein ligand. In the latter case, the LMW ligand is incorporated into the DNIC that produce an EPR signal with an axially symmetrical tensor of the g-factor (g = 2.03) [61].

In this work, FERH overexpression (K562/FERH cells) was used as a strategy to promote the formation of larger and more stable HMWDNICs to investigate their distinctive properties and characteristics. The EPR signals recorded in wild-type K562 cells or K562/FERH cells differed substantially (Figure 9). Comparison of spectra showed that at 77K the EPR signal of DNICs in K562/FERH cells showed a rhombic symmetry with g-factors 2.05, 2.03 and 2.014. This symmetry was lower than the one observed in the wild-type K562 cells, which signal showed the axial symmetry. Interestingly, the shape and g-factor symmetry of EPR signals of wild type K562 cells in which the physiological proteolysis was inhibited by NH_4CL treatment changed from axial to rhombic. The contribution of rhombic signal increased as inhibition progressed, while for untreated cells the axial signal predominated. After 4h incubation, the EPR signal showed rhombic symmetry with g-factors 2.05, 2.03 and 2.014. As stated in the literature, this type of spectral shape is associated with the presence in the complex of two different ligands: thiol and non-thiol descended from one molecule [35,67]. The rhombic g-tensor symmetry of DNIC EPR spectrum is observed for HMWDNICs with proteins. This might suggest that HMWDNICs were visible in the cells after incubation with NH_4Cl, while the LMWDNICs associated signal predominated in cells before proteolysis inhibition. We speculate that stability of HMWDNICs is higher than that of LMWDNICs, but formation of LMWDNICs is necessary for synthesis of HMWDNICs. This would explain decrease of signal intensity observed on Figure 10 and the absence of DNICs formation in cells in which the inhibition of proteolysis was complete (see Figure 3).
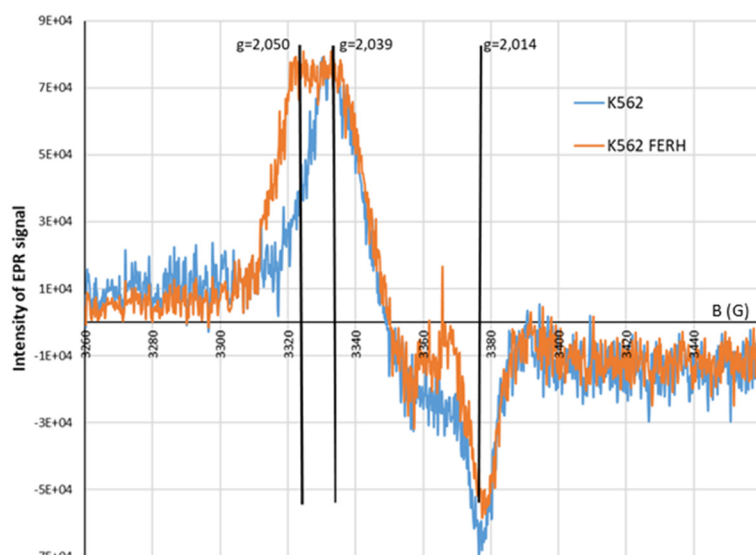
Figure 9. EPR spectra: K562 cells K562 cells overexpressing the heavy chain of ferritin (FERH). The cells were treated with 70 µM DEANO).
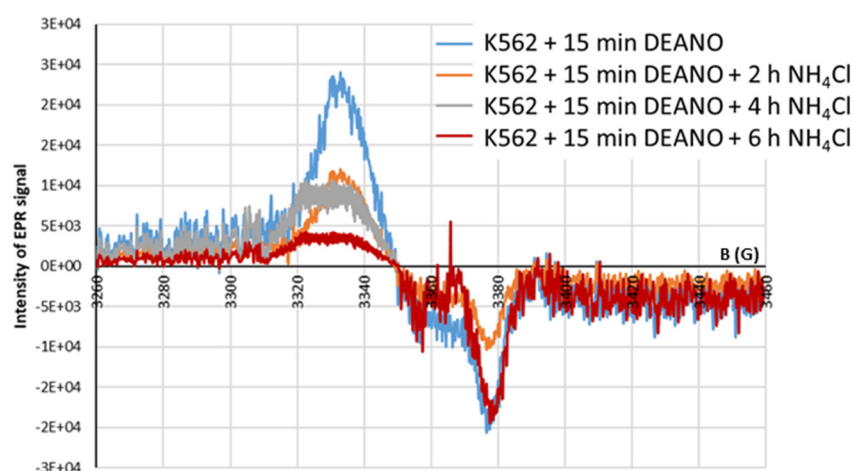
Figure 10. Shape of EPR spectra. Inhibition of EPR signal induction in K562 cells incubated with 10mM NH$_4$Cl for 2, 4, and 6 h and then treated with 70µM DEANO for 15 min at 37°C.

4. Conclusions

The study provides significant insights into the formation of DNICs in vivo and the role of different ligands in this process. Inhibition of lysosomal proteolysis by ammonium chloride led to a time-dependent decrease in DNICs formation, indicating that proteins degraded in lysosomes are an important source of DNIC components. This was confirmed by the use of two different inhibitors of protein degradation in lysosomes and cytosol, namely ALLM and leupeptin. The treatment resulted in even stronger inhibition of DNICs formation. In line, inhibition of protein degradation in proteasome by LAC almost entirely stopped DNICs biosynthesis. Finally, total proteolysis inhibition using ALLN or MG-262, which inhibit various proteases, prevented DNICs formation entirely. Altogether, the presented results underscore the critical importanceof protein degradation, both lysosomal and proteasomal in DNIC biosynthesis.

Furthermore, the study revealed only limited contribution of glutathione (GSH), a low molecular weight thiol, in DNICs biosynthesis. Modulation of GSH level only slightly affected DNICs formation, indicating a minor role of GSH in cellular DNIC formation. Cell fractionation

demonstrated that DNIC signal was more intense in high-molecular-weight fractions of cytosol, further supporting the role of larger ligands, such as proteins, in DNICs stabilization.

The study revealed also a distinct EPR signal with rhombic symmetry in ferritin-overexpressing cells, suggesting the formation of more stable DNICs with large ferritin molecules, incorporating two different ligands in the coordination zone. In contrast, in wild-type K562 cells, EPR signal was of an axial symmetry implying more symmetrical environment around the unpaired electron, or more likely, a faster rotation of a paramagnetic species due to the lower molecular mass of ligands. It is proposed that stability of HMWDNICs is higher than that of LMWDNICs, however formation of LMWDNICs is necessary for the synthesis of HMWDNICs.

In summary, this research provides valuable insights into the role of lysosomal and proteasomal proteolysis, as well as the impact of GSH levels and molecular ligands in the synthesis of DNICs. The study sheds light on the distinct effects of different proteolytic inhibitors and highlights the importance of larger ligands, especially proteins, in DNICs formation. Understanding these mechanisms is essential for comprehending cellular redox regulation and metal-ion homeostasis. The findings may have implications for developing novel therapeutic approaches targeting metal-ion metabolism and for understanding redox signaling in various pathologies related to oxidative stress and altered metal-ion balance.

List of Abbreviations

ALLM	N-Acetyl-L-leucyl-L-leucyl-L-methioninal (lysosome inhibitor)
ATPases	class of enzymes that catalyze hydrolysis of adenosine triphosphate
BSO	D,L-buthionine [S,R]-sulfoximine
DEANO	2-(N,N- Diethyloamino)-diazenolate-2-oxide
DNICs	dinitrosyl iron complexes
EDTA	ethylenediaminetetraacetic acid
EPR	electron paramagnetic resonance
FERH	heavy chain of ferritin
GSH	glutathione
HMWDNICs	dinitrosyl iron complexes with high-molecular-weight ligands
His	histidine
HFS	hyperfine structure
LMWDNICs	dinitrosyl iron complexes with low-molecular-weight ligands
LAC	lactacystin (proteasome inhibitor)

LEUPT	leupeptin (lysosome inhibitor)
MG-101	N-Acetyl-L-leucyl-L-leucyl-L-norleucinal (calpain, lysosome and proteasome inhibitor)
MG-132	Z-Leu-Leu-Leu-al (proteasome inhibitor)
MG-262	Z-Leu-Leu-Leu-B(OH)2 (calpain, lysosome and proteasome inhibitor)
NAC	N-acetylcysteine
PBS	phosphate-buffered saline

References

1. *Nitric Oxide in Transplant Rejection and Anti-Tumor Defense*; Lukiewicz, S., Zweier, J.L., Eds.; Kluwer Academic Publishers: Boston, 1998; ISBN 978-0-7923-8389-5.

2. Ueno, T.; Yoshimura, T. The Physiological Activity and In Vivo Distribution of Dinitrosyl Dithiolato Iron Complex. *Japanese Journal of Pharmacology* **2000**, *82*, 95–101, doi:10.1254/jjp.82.95.

3. Hickok, J.R.; Sahni, S.; Shen, H.; Arvind, A.; Antoniou, C.; Fung, L.W.M.; Thomas, D.D. Dinitrosyliron Complexes Are the Most Abundant Nitric Oxide-Derived Cellular Adduct: Biological Parameters of Assembly and Disappearance. *Free Radical Biology and Medicine* **2011**, *51*, 1558–1566.

4. Vanin, A.F.; Malenkova, I.V.; Serezhenkov, V.A. Iron Catalyzes Both Decomposition and Synthesis ofS-Nitrosothiols: Optical and Electron Paramagnetic Resonance Studies. *Nitric Oxide* **1997**, *1*, 191–203, doi:10.1006/niox.1997.0122.

5. Thomas, D.D.; Corey, C.; Hickok, J.; Wang, Y.; Shiva, S. Differential Mitochondrial Dinitrosyliron Complex Formation by Nitrite and Nitric Oxide. *Redox Biology* **2018**, *15*, 277–283, doi:10.1016/j.redox.2017.12.007.

6. Fitzpatrick, J.; Kim, E. Synthetic Modeling Chemistry of Iron–Sulfur Clusters in Nitric Oxide Signaling. *Acc. Chem. Res.* **2015**, *48*, 2453–2461, doi:10.1021/acs.accounts.5b00246.

7. Crack, J.C.; Le Brun, N.E. Biological Iron-Sulfur Clusters: Mechanistic Insights from Mass Spectrometry. *Coordination Chemistry Reviews* **2021**, *448*, 214171, doi:10.1016/j.ccr.2021.214171.

8. Lewandowska, H.; Kalinowska, M.; Brzoska, K.; Wojciuk, K.; Wojciuk, G.; Kruszewski, M. Nitrosyl Iron Complexes--Synthesis, Structure and Biology. *Dalton Trans.* **2011**, *40*, 8273–8289, doi:10.1039/c0dt01244k.

9. Moënne-Loccoz, P. Spectroscopic Characterization of Heme Iron–Nitrosyl Species and Their Role in NO Reductase Mechanisms in Diiron Proteins. *Nat Prod Rep* **2007**, *24*, 610–620, doi:10.1039/b604194a.

10. Dong, H.T.; Speelman, A.L.; Kozemchak, C.E.; Sil, D.; Krebs, C.; Lehnert, N. The Fe 2 (NO) 2 Diamond Core: A Unique Structural Motif In Non-Heme Iron–NO Chemistry. *Angew. Chem. Int. Ed.* **2019**, *58*, 17695–17699, doi:10.1002/anie.201911968.

11. Dong, H. Synthesis and Reactivity of Non-Heme Iron-Nitrosyl Complexes That Model the Active Sites of NO Reductases. **2021**, doi:10.7302/2834.

12. Thomas, D.D.; Corey, C.; Hickok, J.; Wang, Y.; Shiva, S. Differential Mitochondrial Dinitrosyliron Complex Formation by Nitrite and Nitric Oxide. *Redox Biology* **2018**, *15*, 277–283, doi:10.1016/j.redox.2017.12.007.

13. Medvedeva, V.A.; Ivanova, M.V.; Shumaev, K.B.; Dudylina, A.L.; Ruuge, E.K. Generation of Superoxide Radicals by Heart Mitochondria and the Effects of Dinitrosyl Iron Complexes and Ferritin. *BIOPHYSICS* **2021**, *66*, 603–609, doi:10.1134/S0006350921040138.

14. Mukosera, G.T.; Principe, P.; Mata-Greenwood, E.; Liu, T.; Schroeder, H.; Parast, M.; Blood, A.B. Iron Nitrosyl Complexes Are Formed from Nitrite in the Human Placenta. *Journal of Biological Chemistry* **2022**, *298*, 102078, doi:10.1016/j.jbc.2022.102078.

15. Singh, N.; Bhatla, S.C. Heme Oxygenase-Nitric Oxide Crosstalk-Mediated Iron Homeostasis in Plants under Oxidative Stress. *Free Radical Biology and Medicine* **2022**, *182*, 192–205, doi:10.1016/j.freeradbiomed.2022.02.034.

16. Burgova, E.N.; Tkachev, N.A.; Paklina, O.V.; Mikoyan, V.D.; Adamyan, L.V.; Vanin, A.F. The Effect of Dinitrosyl Iron Complexes with Glutathione and S-Nitrosoglutathione on the Development of Experimental Endometriosis in Rats: A Comparative Studies. *European Journal of Pharmacology* **2014**, *741*, 37–44, doi:10.1016/j.ejphar.2014.07.017.

17. Vladimir, T.; Anatoly, O.; Larisa, I.; Vladimir, P.; Anna, D.; Anna, O. Hypothetical Mechanism of Light Action on Nitric Oxide Physiological Effects. *Lasers Med Sci* **2021**, *36*, 1389–1395, doi:10.1007/s10103-020-03169-x.

18. Vanin, A.F.; Mikoyan, V.D.; Borodulin, R.R.; Burbaev, D.S.; Kubrina, L.N. Dinitrosyl Iron Complexes with Persulfide Ligands: EPR and Optical Studies. *Appl Magn Reson* **2016**, *47*, 277–295, doi:10.1007/s00723-015-0744-6.

19. Vanin, A.F. *Dinitrosyl Iron Complexes as a "Working Form" of Nitric Oxide in Living Organisms*; Cambridge Scholars Publishing, 2019; ISBN 1-5275-4075-8.

20. Chenais, B.; Morjani, H.; Drapier, J.C. Impact of Endogenous Nitric Oxide on Microglial Cell Energy Metabolism and Labile Iron Pool. *J.Neurochem.* **2002**, *81*, 615–623.

21. Jasid, S.; Simontacchi, M.; Puntarulo, S. Exposure to Nitric Oxide Protects against Oxidative Damage but Increases the Labile Iron Pool in Sorghum Embryonic Axes. *J.Exp.Bot.* **2008**, ern235.

22. Kruszewski, M.; Lewandowska, H.; Starzyäski, R.; Bartlomiejczyk, T.; Iwanenko, T.; Lipinski, P. Role of Labile Iron Pool in Nitric Oxide-Induced Genotoxicity,.; August 25 2003.

23. Kruszewski, M.; Lewandowska, H.; Starzyäski, R.; Bartlomiejczyk, T.; Iwanenko, T.; Drapier, J.C.; Lipinski, P. The Role of Labile Iron Pool and Dinitrosyl Iron Complexes in Nitric Oxide Genotoxicity.; July 3 2004.

24. Kruszewski, M.; Lewandowska, H.; Starzynski, R.; Bartomiejczyk, T.; Iwanenko, T.; Drapier, J.; Lipinski, P. Labile Iron Pool, Dinitrosyl Iron Complexes and Nitric Oxide Genotoxicity.; PERGAMON-ELSEVIER SCIENCE LTD THE BOULEVARD, LANGFORD LANE, KIDLINGTON, OXFORD OX5 1GB, ENGLAND, 2004; Vol. 36, pp. S52–S52.

25. Lipinski, P.; Starzynski, R.R.; Drapier, J.C.; Bouton, C.; Bartlomiejczyk, T.; Sochanowicz, B.; Smuda, E.; Gajkowska, A.; Kruszewski, M. Induction of Iron Regulatory Protein 1 RNA-Binding Activity by Nitric Oxide Is Associated with a Concomitant Increase in the Labile Iron Pool: Implications for DNA Damage. *Biochem.Biophys.Res.Commun.* **2005**, *327*, 349–355.

26. Lewandowska, H. Coordination Chemistry of Nitrosyls and Its Biochemical Implications. In *Nitrosyl Complexes in Inorganic Chemistry, Biochemistry and Medicine I*; Mingos, D.M.P., Ed.; Structure and Bonding; Springer Berlin Heidelberg, 2014; Vol. 153, pp. 45–114 ISBN 978-3-642-41186-1.

27. Lewandowska, H.; Sadło, J.; Męczyńska, S.; Stępkowski, T.M.; Wójciuk, G.; Kruszewski, M. Formation of Glutathionyl Dinitrosyl Iron Complexes Protects against Iron Genotoxicity. *Dalton Transactions* **2015**, *44*, 12640–12652.

28. Lewandowska, H.; Męczyńska-Wielgosz, S.; Sikorska, K.; Sadło, J.; Dudek, J.; Kruszewski, M. LDL Dinitrosyl Iron Complex: A New Transferrin-independent Route for Iron Delivery in Hepatocytes. *BioFactors* **2018**, *44*, 192–201.

29. Rogers, P.A.; Ding, H. L-Cysteine-Mediated Destabilization of Dinitrosyl Iron Complexes in Proteins. *J.Biol.Chem.* **2001**, *276*, 30980–30986.

30. Rogers, P.A.; Eide, L.; Klungland, A.; Ding, H. Reversible Inactivation of E. Coli Endonuclease III via Modification of Its [4Fe-4S] Cluster by Nitric Oxide. *DNA Repair (Amst)* **2003**, *2*, 809–817.

31. Tonzetich, Z.J.; Do, L.H.; Lippard, S.J. Dinitrosyl Iron Complexes Relevant to Rieske Cluster Nitrosylation. *Journal of the American Chemical Society* **2009**, *131*, 7964–7965.

32. Tonzetich, Z.J.; McQuade, L.E.; Lippard, S.J. Detecting and Understanding the Roles of Nitric Oxide in Biology. *Inorg.Chem.* **2010**, *49*, 6338–6348.

33. Harrop, T.C.; Tonzetich, Z.J.; Reisner, E.; Lippard, S.J. Reactions of Synthetic [2Fe-2S] and [4Fe-4S] Clusters with Nitric Oxide and Nitrosothiols. *Journal of the American Chemical Society* **2008**, *130*, 15602–15610, doi:10.1021/ja8054996.

34. Tinberg, C.E.; Tonzetich, Z.J.; Wang, H.; Do, L.H.; Yoda, Y.; Cramer, S.P.; Lippard, S.J. Characterization of Iron Dinitrosyl Species Formed in the Reaction of Nitric Oxide with a Biological Rieske Center. *Journal of the American Chemical Society* **2010**, *132*, 18168–18176.

35. Vanin, A.F. Dinitrosyl Iron Complexes and S-Nitrosothiols Are Two Possible Forms for Stabilization and Transport of Nitric Oxide in Biological Systems. *Biochemistry (Mosc)* **1998**, *63*, 782–793.

36. Lewandowska, H.; Kalinowska, M.; Brzóska, K.; Wójciuk, K.; Wójciuk, G.; Kruszewski, M. Nitrosyl Iron Complexes—Synthesis, Structure and Biology. *Dalton Transactions* **2011**, *40*, 8273–8289.

37. Lewandowska-Siwkiewicz, H.; Kruszewski, M. *Dinitrosyl Iron Complexes in Biological Systems*; Poland, 2006; p. 36;.

38. Lewandowska, H.; Męczyńska, S.; Sochanowicz, B.; Sadło, J.; Kruszewski, M. Crucial Role of Lysosomal Iron in the Formation of Dinitrosyl Iron Complexes in Vivo. *Journal of Biological Inorganic Chemistry* **2007**, *12*, 345–352.

39. Ueno, T.; Suzuki, Y.; Fujii, S.; Vanin, A.F.; Yoshimura, T. *In Vivo* Distribution and Behavior of Paramagnetic Dinitrosyl Dithiolato Iron Complex in the Abdomen of Mouse. *Free Radical Research* **1999**, *31*, 525–534, doi:10.1080/10715769900301101.

40. Timoshin, A.A.; Vanin, A.F.; Orlova, T.R.; Sanina, N.A.; Ruuge, E.K.; Aldoshin, S.M.; Chazov, E.I. Protein-Bound Dinitrosyl–Iron Complexes Appearing in Blood of Rabbit Added with a Low-Molecular Dinitrosyl–Iron Complex: EPR Studies. *Nitric Oxide* **2007**, *16*, 286–293, doi:10.1016/j.niox.2006.09.005.

41. Bradford, M.M. A Rapid and Sensitive Method for the Quantitation of Microgram Quantities of Protein Utilizing the Principle of Protein-Dye Binding. *Analytical Biochemistry* **1976**, *72*, 248–254, doi:10.1016/0003-2697(76)90527-3.

42. Barhoumi, R.; Bailey, R.H.; Burghardt, R.C. Kinetic Analysis of Glutathione in Anchored Cells with Monochlorobimane. *Cytometry* **1995**, *19*, 226–234, doi:10.1002/cyto.990190306.

43. Shumaev, K.B.; Dudylina, A.L.; Ivanova, M.V.; Pugachenko, I.S.; Ruuge, E.K. Dinitrosyl Iron Complexes: Formation and Antiradical Action in Heart Mitochondria. *BioFactors* **2018**, *44*, 237–244, doi:10.1002/biof.1418.

44. Lu, Q.; Mellgren, R.L. Calpain Inhibitors and Serine Protease Inhibitors Can Produce Apoptosis in HL-60 Cells. *Archives of Biochemistry and Biophysics* **1996**, *334*, 175–181, doi:10.1006/abbi.1996.0443.

45. Hiwasa, T.; Sawada, T.; Sakiyama, S. Cysteine Proteinase Inhibitors and *Ras* Gene Products Share the Same Biological Activities Including Tranforming Activity toward NIH3T3 Mouse Fibroblasts and the Differentiation-Inclucing Activity toward PC12 Rat Pheochromocytoma Cells. *Carcinogenesis* **1990**, *11*, 75–80, doi:10.1093/carcin/11.1.75.

46. Kurinov, I.V.; Harrison, R.W. Two Crystal Structures of the Leupeptin-Trypsin Complex. *Protein Sci* **1996**, *5*, 752–758.

47. Yang, Y.; Hu, L.; Zheng, H.; Mao, C.; Hu, W.; Xiong, K.; Wang, F.; Liu, C. Application and Interpretation of Current Autophagy Inhibitors and Activators. *Acta Pharmacol Sin* **2013**, *34*, 625–635, doi:10.1038/aps.2013.5.

48. Mindell, J.A. Lysosomal Acidification Mechanisms. *Annu. Rev. Physiol.* **2012**, *74*, 69–86, doi:10.1146/annurev-physiol-012110-142317.

49. Craiu, A.; Gaczynska, M.; Akopian, T.; Gramm, C.F.; Fenteany, G.; Goldberg, A.L.; Rock, K.L. Lactacystin and Clasto-Lactacystin β-Lactone Modify Multiple Proteasome β-Subunits and Inhibit Intracellular Protein Degradation and Major Histocompatibility Complex Class I Antigen Presentation. *Journal of Biological Chemistry* **1997**, *272*, 13437–13445, doi:10.1074/jbc.272.20.13437.

50. Squier, M.K.T.; Miller, A.C.K.; Malkinson, A.M.; Cohen, J.J. Calpain Activation in Apoptosis. *J. Cell. Physiol.* **1994**, *159*, 229–237, doi:10.1002/jcp.1041590206.

51. Goldberg, A.L. Development of Proteasome Inhibitors as Research Tools and Cancer Drugs. *Journal of Cell Biology* **2012**, *199*, 583–588, doi:10.1083/jcb.201210077.

52. Fuertes, G.; De Llano, J.J.M.; Villarroya, A.; Rivett, A.J.; Knecht, E. Changes in the Proteolytic Activities of Proteasomes and Lysosomes in Human Fibroblasts Produced by Serum Withdrawal, Amino-Acid Deprivation and Confluent Conditions. *Biochemical Journal* **2003**, *375*, 75–86, doi:10.1042/bj20030282.

53. Lee, D.H.; Goldberg, A.L. Proteasome Inhibitors: Valuable New Tools for Cell Biologists. *Trends in Cell Biology* **1998**, *8*, 397–403, doi:10.1016/S0962-8924(98)01346-4.

54. Kageyama, M.; Ota, T.; Sasaoka, M.; Katsuta, O.; Shinomiya, K. Chemical Proteasome Inhibition as a Novel Animal Model of Inner Retinal Degeneration in Rats. *PLoS ONE* **2019**, *14*, e0217945, doi:10.1371/journal.pone.0217945.

55. Berndtsson, M.; Beaujouin, M.; Rickardson, L.; Havelka, A.M.; Larsson, R.; Westman, J.; Liaudet-Coopman, E.; Linder, S. Induction of the Lysosomal Apoptosis Pathway by Inhibitors of the Ubiquitin-proteasome System. *Intl Journal of Cancer* **2009**, *124*, 1463–1469, doi:10.1002/ijc.24004.

56. Frase, H.; Hudak, J.; Lee, I. Identification of the Proteasome Inhibitor MG262 as a Potent ATP-Dependent Inhibitor of the *Salmonella Enterica* Serovar Typhimurium Lon Protease. *Biochemistry* **2006**, *45*, 8264–8274, doi:10.1021/bi060542e.

57. Pujols, L.; Fernández-Bertolín, L.; Fuentes-Prado, M.; Alobid, I.; Roca-Ferrer, J.; Agell, N.; Mullol, J.; Picado, C. Proteasome Inhibition Reduces Proliferation, Collagen Expression, and Inflammatory Cytokine Production in Nasal Mucosa and Polyp Fibroblasts. *J Pharmacol Exp Ther* **2012**, *343*, 184–197, doi:10.1124/jpet.111.190710.

58. Mehdi, S. Cell-Penetrating Inhibitors of Calpain. *Trends in Biochemical Sciences* **1991**, *16*, 150–153, doi:10.1016/0968-0004(91)90058-4.

59.   Barrett, D. Proteinase and Peptidase Inhibition: Recent Potential Targets for Drug Development. *Drug Discovery Today* **2002**, *7*, 1124, doi:10.1016/S1359-6446(02)02402-9.

60.   Vanin, A.F. Dinitrosyl Iron Complexes and S-Nitrosothiols Are Two Possible Forms for Stabilization and Transport of Nitric Oxide in Biological Systems. *Biochemistry (Mosc.)* **1998**, *63*, 782–793.

61.   Vanin, A.F.; Serezhenkov, V.A.; Mikoyan, V.D.; Genkin, M.V. The 2.03 Signal as an Indicator of Dinitrosyl-Iron Complexes with Thiol-Containing Ligands. *Nitric.Oxide.* **1998**, *2*, 224–234.

62.   Lipinski, P.; Lewandowska, H.; Drapier, J.C.; Starzyäski, R.; Bartlomiejczyk, T.; Kruszewski, M. Increase in Labile Iron Pool (LIP) Level and Generation of EPR-Detectable Dinitrosyl-Non-Heme Iron Complexes in L5178Y Cells Exposed to Nitric Oxide. Possible Role of LIP as a Source of Iron for DNIC Formation.; September 5 2003.

63.   Lee, M.; Arosio, P.; Cozzi, A.; Chasteen, N.D. Identification of the EPR-Active Iron-Nitrosyl Complexes in Mammalian Ferritins. *Biochemistry* **1994**, *33*, 3679–3687.

64.   Lewandowska, H.; Stępkowski, T.M.; Sadło, J.; Wójciuk, G.P.; Wójciuk, K.E.; Rodger, A.; Kruszewski, M. Coordination of Iron Ions in The Form of Histidinyl Dinitrosyl Complexes Does Not Prevent Their Genotoxicity. *Bioorganic & Medicinal Chemistry* **2012**.

65.   Cesareo, E.; Parker, L.J.; Pedersen, J.Z.; Nuccetelli, M.; Mazzetti, A.P.; Pastore, A.; Federici, G.; Caccuri, A.M.; Ricci, G.; Adams, J.J.; et al. Nitrosylation of Human Glutathione Transferase P1-1 with Dinitrosyl Diglutathionyl Iron Complex in Vitro and in Vivo. *J.Biol.Chem.* **2005**, *280*, 42172–42180.

66.   De Maria, F.; Pedersen, J.Z.; Caccuri, A.M.; Antonini, G.; Turella, P.; Stella, L.; Lo Bello, M.; Federici, G.; Ricci, G. The Specific Interaction of Dinitrosyl-Diglutathionyl-Iron Complex, a Natural NO Carrier, with the Glutathione Transferase Superfamily: Suggestion for an Evolutionary Pressure in the Direction of the Storage of Nitric Oxide. *J.Biol.Chem.* **2003**, *278*, 42283–42293.

67.   Vanin, A.F. Physico-Chemistry of Dinitrosyl Iron Complexes as a Determinant of Their Biological Activity. *IJMS* **2021**, *22*, 10356, doi:10.3390/ijms221910356.